Hindawi
Journal of Nanomaterials
Volume 2021, Article ID 6244874, 13 pages
https://doi.org/10.1155/2021/6244874

Research Article

Design, Simulation, and Analysis of Micro/Nanoelectromechanical System Rotational Devices

A. R. Kalaiarasi,[1] T. Deepa,[2] S. Angalaeswari,[2] D. Subbulekshmi,[2] and Raja Kathiravan[3]

[1]*Department of Electronics and Instrumentation, Saveetha Engineering College, Chennai, India*
[2]*School of Electrical Engineering, Vellore Institute of Technology, Chennai, India*
[3]*School of Mechanical Engineering, Bahir Dar University, Bahir Dar, Ethiopia 6000*

Correspondence should be addressed to T. Deepa; deepa.t@vit.ac.in, S. Angalaeswari; angalaeswari.s@vit.ac.in, and Raja Kathiravan; kathirrk3000@gmail.com

Received 8 September 2021; Revised 29 September 2021; Accepted 21 October 2021; Published 9 November 2021

Academic Editor: Lakshmipathy R

This work is focused on design and simulation of microelectromechanical system (MEMS)/nanoelectromechanical system (NEMS) rotational devices such as micro/nanothermal rotary actuator and micro/nanogear. MEMS/NEMS technologies have allowed the development of advanced miniaturized rotational devices. MEMS/NEMS-based thermal actuator is a scaled version of movable device which will produce amplified motion when it is subjected to thermal forces. One of the applications of such thermal micro/nanoactuator is integrating it into micro/nanomotor that makes a thermal actuated micro/nanomotor. In this work, design and simulation of micro/nanothermal rotary actuator are done using MEMS/NEMS technology. Stress, current density, and temperature analysis are done for microthermal rotary actuator. The performance of the device is observed by varying the dimensions and materials such as silicon and polysilicon. Stress analysis is used to calculate the yield strength of the material. Current density is used to calculate the safer limit of the material. Temperature analysis is used to calculate the melting point of the material. Also, in this work, design and simulation of microgear have been done. Micro/nanogears are devices that can be used to improve motion performance. The essential is that it transmits rotational motion to a different axis.

1. Introduction

MEMS technology is a representation of microscopic implementations of sensors and actuators which are fabricated using microfabrication techniques. MEMS/NEMS devices generally fall in the range between 1 and 1000 nanometers in size. MEMS/NEMS technologies are developed for the fabrication of integrated circuits (IC). MEMS/NEMS devices can be categorized in to sensors and actuators in μ scale, which can be further used in macroworld. They have wide applications in the fields as diverse as microsatellites, automotive, aerospace, telecommunication, biomedical, wind tunnel instrumentation etc. MEMS/NEMS has strong multidisciplinary character. MEMS/NEMS devices have the following advantages like less power consumption, small size, improved performance, increasing reliability, lesser weight, and less cost than devices which are working on similar fundamental principle in macrosize. MEMS/NEMS-based devices are fabricated using IC fabrication techniques along with special techniques to fabricate three dimensional (3D) structures. It has high precision and high aspect ratio. It scales the size of the device without changing the property of the materials.

MEMS-based thermal actuator is an electromechanically actuated device which works based on Joules' law of electrothermal heating. Amplification of thermal force may be done in design of thermal actuator. Electrothermal actuator fabricated using single crystal silicon or polysilicon as a compliance structure. Atre and Boedo [1] analyzed the variation of tip deflection of actuator with respect to the applied

voltage. The thermal behavior of the polysilicon material and its relationship in the calculation of deflection by analytical methods are studied. The experimental and simulation results of six different actuator designs are compared. At high voltages, the finite element model overestimates experimentally determined values. Thermal conductivity of polysilicon plays an important role in predicting actuator deflection. Geisberger et al. [2] discussed about the influence of dopant concentration in electrical and thermal conductivity. Investigating the static and transient response of the thermal actuator at different excitation frequency and voltage, the simulated and measured data are compared. Relatively poor fit of simulation data using constant conductivities explains the importance of thermal properties of the material. Heo and Kim [3, 4] designed a robust to maximize the actuator deflection with respect to applied voltage and baseline design by the topology optimization method. Optimize the thermal actuator design, which is robust to noise factors.

Heo and Kim [5] described the optimal design to maximize the rotation angle of the actuator for fixed input power. Element connectivity parameterization formulation method is used to eradicate numerical instabilities. Haefner et al. [6] evaluated the lifetime evaluation of microgears, which depend on the geometry shape deviations (tooth deformation) and finite element model-based prognostic method. Islam and Islam [7] analyzed the finite element method of stress, contact stress, and bending stress for spur gears, used in the hybrid vehicle power transmission system. Arefin et al. [8] implemented both PV module and wind turbine in internal combustion engine-based vehicle. Wind turbine blade design was simulated using ANSYS CFD. Jin et al. [9] designed impact of upstream deflector parameters (rotor distance influence, width influence, distance influence, and height influence) in vertical axis wind turbines. Compare with the simulated and experimental results with and without deflector, Deflector reduces negative torque and increases efficiency of wind turbine.

Arefin and Islam [10] studied about noise characteristics and emission characteristics of micro gas turbine, which is used as range extender for electric truck. Suitable temperature of operating the micro gas turbine for maximum power is studied. Noise reduction methods are proposed at higher speed, output power is increased, and vibration (noise) and CO emission are reduced. Karbosi et al. [11] compared the properties of two microactuators such as distribution of temperature, power consumed, and actuation of two microactuators. Analysis of two designs is like design a—different beam lengths and design B—different beam sections and flexure part, to produce maximum deflection. GA Optimal design produces 70% increase in tip deflection. Lo et al. [12] modeled the electrothermal-mechanical system into a combination of electrical, thermal, and mechanical model using the lumped model technique. Deflection and frequency bandwidth are analyzed to attain and determine static gain.

Dhinakaran et al. [13] demonstrated the combination of electrothermal and electrostatic actuation mechanisms. It gives pull-in behavior at low voltage and makes hybrid actuator and hybrid bidirectional actuator perfect for switching

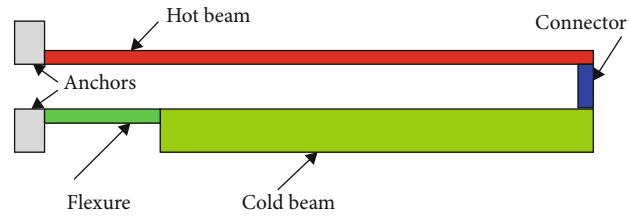

Figure 1: A-symmetric (bimorph).

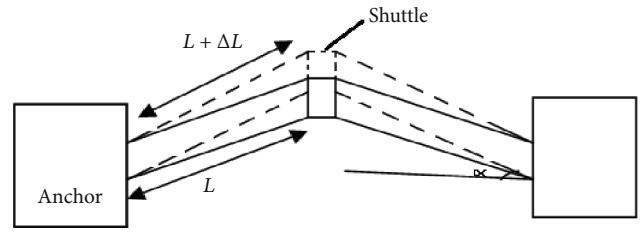

Figure 2: Chevron single beam actuator.

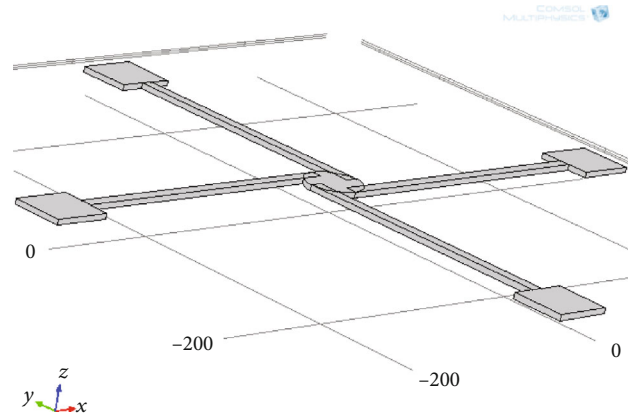

Figure 3: Microthermal rotary actuator structure.

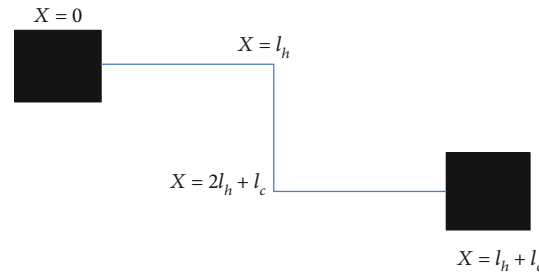

Figure 4: 1D of actuator.

applications. Chiorean et al. [14] analyzed the effect of geometrical parameters on the output force of Chevron actuators. The authors also considered the effect of thermal expansion of substrate. It studies about the impact of substrate silicon deformation due to forces in anchors and thermal expansion of substrate silicon or effect of central shaft expansion in actuator displacement. Suocheng et al. [15] studied bimetal film thermal expansion-based microthermal actuator variation of actuator displacement at

Table 1: Parameters used.

Sl. No.	Parameters	Values
1.	Coefficient of thermal expansion of polysilicon (α)	2.7×10^{-6} K^{-1}
2.	Electrical specific resistance of polysilicon at room temperature (ρ_0)	2×10^{-3} Ω – cm
3.	Thermal conductivity of polysilicon (k_p)	32 W-m^{-1}-K^{-1}
4.	Thermal conductivity of air (k_a)	0.006 W-m^{-1}-K^{-1}
5.	Thermal conductivity of silicon(k_n)	2.25 W-m^{-1}-K^{-1}
6.	Thickness of polysilicon (t_p)	2000 nm
7.	Thickness of air (t_a)	2000 nm
8.	Thickness (t_{p0})	2000 nm
9.	Thickness of silicon (t_n)	2000 nm

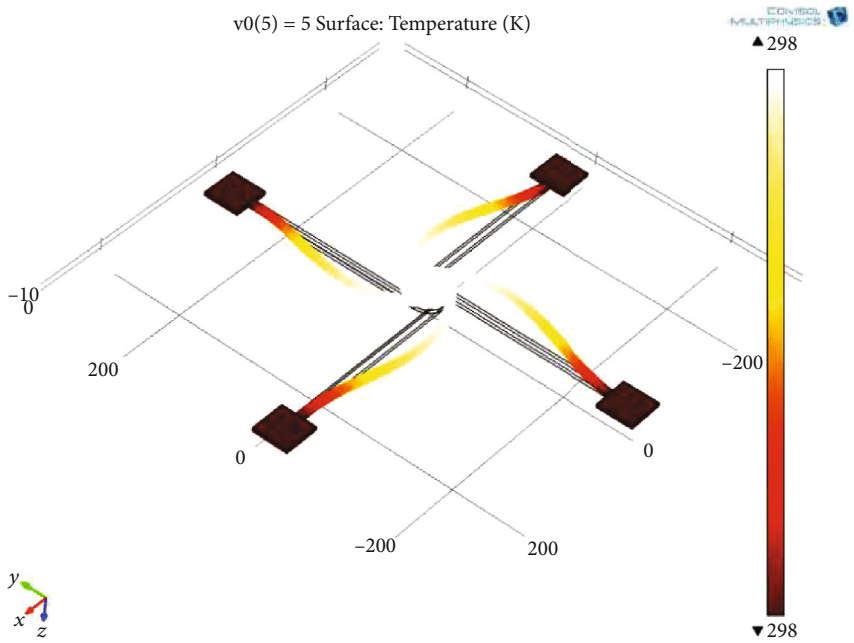

Figure 5: Temperature analysis of silicon (circular disc 5 μm).

different voltage values and temperature ranges. Time taken to achieve maximum displacement (response time) at different voltage levels is also investigated. Potekhina and Wang [16] designed hot and cold arm type actuators where differential thermal expansion is achieved by various geometrical shapes like changing beam shape, modifying electrical parameters like selective doping, modified resistance, or topological parameter changes like multimode or bidirectional operation. Sun et al. [17] explained about the single walled carbon nanotube (SWCNT) electrothermal actuators thermal expansion that is based on the following parameters such as amount of joule heating and coefficient of thermal expansion, induced stress relaxation mechanism and post-secondary curing. Li et al. [18] studied the application of series of V-beam thermal actuator amplification for MEMS applications in specific areas like safety and arming. Yogeshwaran et al. [19] discussed about the temperature distribution dynamics and displacement and its impact on the device dimensions and properties of material and applied

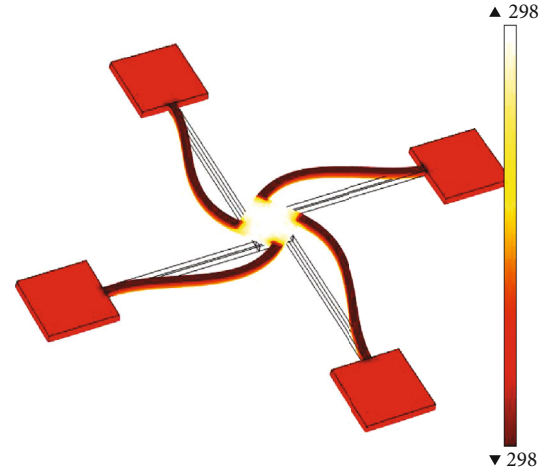

Figure 6: Temperature analysis of silicon (square arm 10 μm).

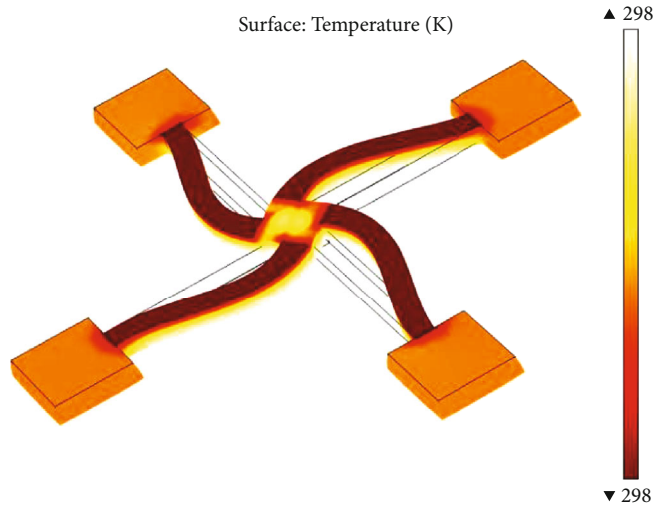

Figure 7: Temperature analysis of silicon (square arm 25 μm).

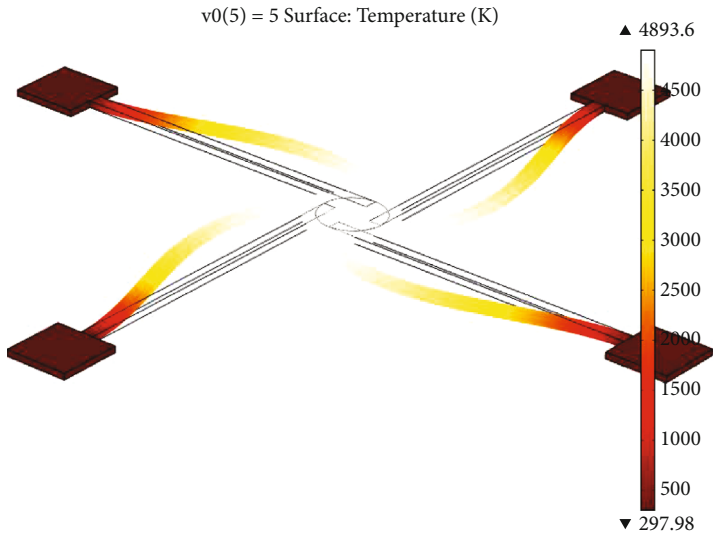

Figure 8: Temperature analysis of polysilicon (circular disc 5 μm).

voltage. Kim et al. [20] designed and fabricated the multilayered structure with platinum heater. Ni-Co-based flexible substrate as thermal bimorph actuators and thermal insulation (isolation) layers are also employed. Ulkir [21] designed bidirectional electrothermal actuator which displaces in two directions. Authors compared the fabrication process of 2 photon polymerization (2PP) and digital light processing (DLP) methods, which are 3D printing techniques. Steiner et al. [22] studied the relation between actuator area and deflection distance based on V-shaped Chevron type beams.

Duzng [23] modeled the V-shaped thermal actuator using ordinary differential equations. Author studied about the thermal inertia of the system, if the applied voltage is in the form of square pulse, the output is in form of concave trapezium. Li et al. [24] discussed the application of thermal actuator in testing the fracture strength of thin films. Voltage is applied to thermal actuator, which creates the thermal expansion; due to thermal expansion force that is created which is used to fracture the test structure. Suryanarayanan et al. [25] compared experimental results, and simulation results are correlated using back propagation neural network. Simulation results fitted with neural network provide a cost-effective model for V-shaped thermal actuator. Gong et al. [26] studied the relation between length of flexure and thermal deflection of bimorph thermal actuator. The author proposes that the length of flexure would not increase the stress on the arm length, and it also increases the lifetime of actuator. López-Walle et al. [27] discussed heat transfer characteristics that are important in improving the performance of thermal actuator. Kim et al. [28] discussed the application of bimorph thermal actuators in rotation control of micromirrors. Two bimorph actuators produce vertical displacement of 25 μm at 10 V, which rotates micromirror by 20°.

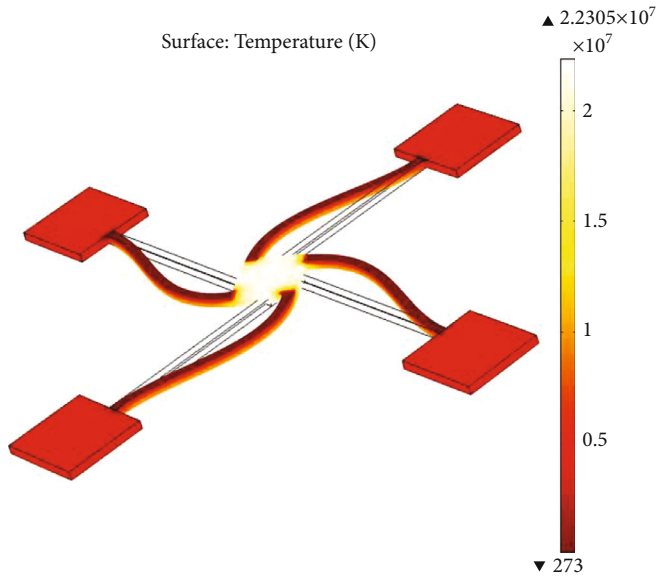

Figure 9: Temperature analysis of polysilicon (square arm 10 μm).

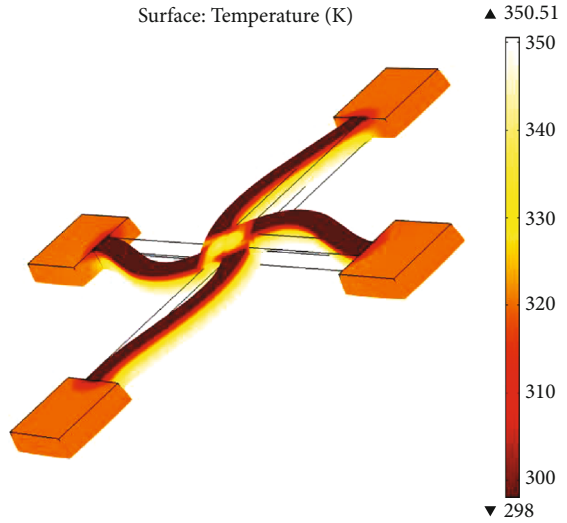

Figure 10: Temperature analysis of polysilicon (square arm 25 μm).

2. Importance of Microthermal Rotary Actuator

Electrostatic actuation and thermal actuation are methods to obtain actuation in MEMS. This method of actuations is very popular since this actuation provides simplicity, fast actuation rates, and low power consumption, and it uses silicon as its material. This type of actuation method is a common method of driving MEMS devices because it is compatible with microfabrication.

Thermal microactuators have the following advantages like higher force, lesser operating voltages, and less susceptibility to adhesion failures compared to electrostatic actuators. Microthermal actuators do require more power, and their switching speeds are limited by cooling times. It produces higher displacement and higher force than electrostatic actuators.

3. Types of Microthermal Rotary Actuator

3.1. A-Symmetric (Bimorph). A bimorph is a microcantilever based thermal actuator used as an actuator or sensor which consists of two metal layers. In some applications, it also has a passive layer between the two active layers. The term bimorph is most commonly used with thermal bimorphs. The first theory about the bending of thermally actuated bimorph was given by Stoney. In Figure 1, schematic diagram of A-symmetric (bimorph) is shown. It has generally a single material. The deflection is produced here due to asymmetry in the shape. This type of thermal actuator is also called as hot-cold beam actuator.

3.2. Symmetric (Bent Beam, Chevron). Chevron-shaped actuators are one of the most popular actuators in the MEMS

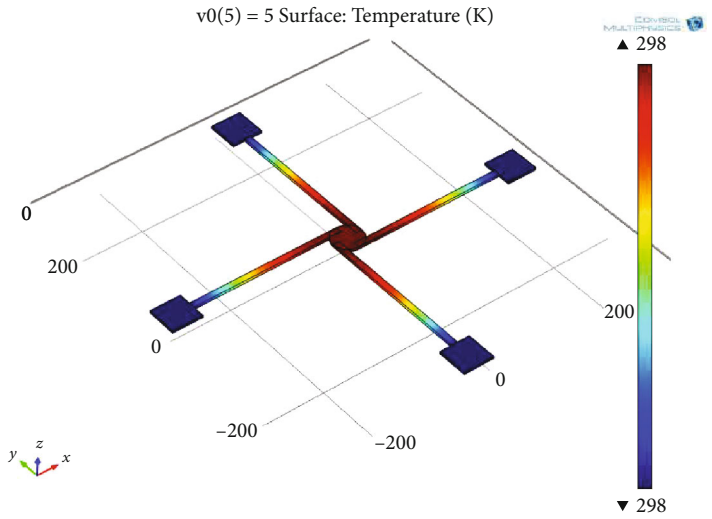

Figure 11: Current density analysis of silicon (circular disc 5 μm).

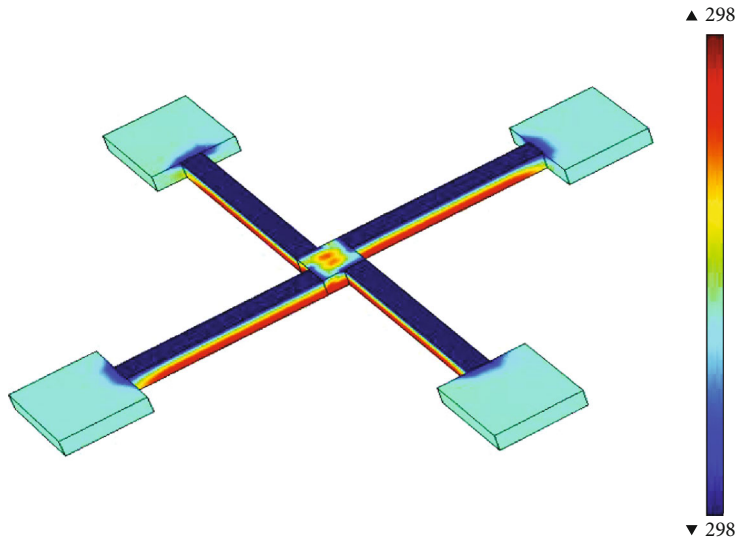

Figure 12: Current density analysis of silicon (square arm 10 μm).

community (also called V-beam thermal actuator). Its principle is based on the thermal expansion of a single material to generate the motion, which is amplified using different geometric constraints. The V-beam thermal actuators are capable of producing high output force for low operating voltage. The output force (displacement) depends on the inclination of the beam. In Figure 2, Chevron beam actuator is shown.

3.3. Designing of Microthermal Rotary Actuator. Designing of microthermal rotary actuator is done using structural mechanics. For designing the microthermal rotary actuator, the important parameters used are materials and dimensions. Finite element method (FEM) software used to design the thermal actuator. Here, COMSOL is used for simulation. The actuator's operation involves three coupled physics phenomena: electric current conduction, heat conduction with heat generation, and structural stresses and strains due to thermal expansion. In COMSOL, the joule heating model uses the heat equation given in equation as the mathematical model for heat transfer in solids.

3.3.1. Dimensions. Microthermal rotary actuator is done using structural differ from varying its length and shape of the cold disc. Length of the hot arm is varies from 500 nm to 2500 nm. Height of the cold beam is 500 nm, and the diameter of the cold beam is 200 nm. Figure 3 shows the microthermal rotary actuator structure.

3.3.2. Materials. Materials used for designing of microthermal rotary actuator are silicon and poly silicon. Each material has a unique property which makes them to use in designing the microthermal rotary actuator.

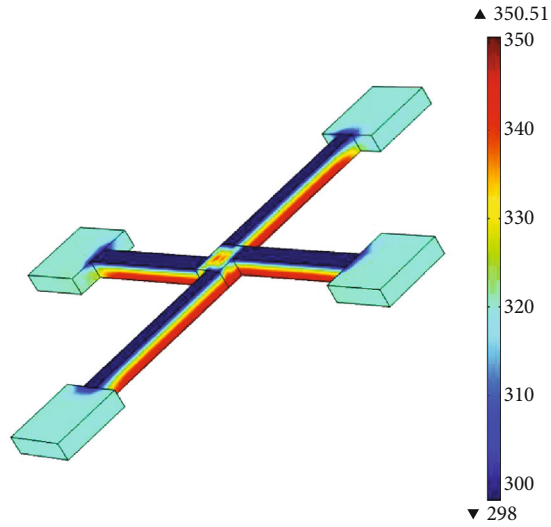

Figure 13: Current density analysis of silicon (square arm 25 μm).

3.4. Theoretical Analysis

3.4.1. Electrothermal Analysis. The above Figure 4 shows the 1D of actuator. According to joule's heating,

rate of heat input = rate of heat going out

$$Q_{\text{in}} + Q_{\text{joule}} = Q_{\text{out,arm}} + Q_{\text{out,sub.}} \tag{1}$$

Since

$$Q_{\text{in}} = -k_p w t_p \left[\frac{dT}{dx}\right]_x ; Q_{\text{joule}} = J^2 \rho w t_p dx,$$
$$Q_{\text{out,arm}} = -k_p w t_p \left[\frac{dT}{dx}\right]_{x+dx} ; Q_{\text{out,sub}} = Sdxw\frac{T - T_{\text{sub}}}{R_T}, \tag{2}$$

where T is the temperature at any given location of the actuator. T_{sub} is the substrate temperature. ρ is the resistivity of material. k_p is the thermal conductivity of material. J is the current density of hot arm or cold disc. S is the shape factor. R_T is the thermal resistance between the device and the substrate.

Substitute above values in Equation (1), and we get

$$-k_p w t_p \left[\frac{dT}{dx}\right]_x + J^2 \rho w t_p dx = -k_p w t_p \left[\frac{dT}{dx}\right]_{x+dx} + Sdxw\frac{T - T_{\text{sub}}}{R_T} \tag{3}$$

Thermal resistance between the device and the substrate is given by

$$R_t = \frac{t_a}{k_a} + \frac{t_{p0}}{k_{p0}} + \frac{t_n}{k_n}, \tag{4}$$

where t_a, $t_{p0,}$ and t_n are the thickness of the element above the polysilicon layer, thickness of polysilayer, and thickness of silicon layer. k_a, k_{p0}, and k_n are the thermal conductivity values of air, polysilicon and silicon, respectively.

Substitute the needed values to Equation (4) from Table 1. After calculating thermal resistance obtained, it is$R_t = 7.7205 \times 10^{-5}$.

Current density is the amount of current by unit area. The current density of hot arm and cold disc is calculated from

$$J_h = \frac{I}{w_p t_p}, \tag{5}$$

$J_c = .$

Using the above equation, the calculated current density value is $J_h = 7.5 \times 10^{11}$ and $J_c = 15 \times 10^{11}$. The calculated values almost match with the values obtained from simulation; so, the device can be able to fabricate.

Shape factor of the hot arm is given by

$$S = \frac{t_p}{w_h}\left[\frac{2t_a}{t_p} + 1\right] + 1. \tag{6}$$

The obtained shape factor is $S = 1.6\,\mu$m.

Resistivity is calculated by using the Van der paw method:

$$\rho = \left(2.971 \times 10^{-2}\right)T + 20.858. \tag{7}$$

At room temperature, the resistivity is $\rho = 21.5\,\mu\Omega$.

Simplifying the Equation (3), we get

$$\frac{d^2T(x)}{dx^2} = \frac{S(T(x) - T_{sub})}{k_p t_p R_T} - \frac{J^2\rho}{k_p}. \tag{8}$$

3.4.2. Rotational Analysis.

$$\Delta \text{Lh} = R\delta. \tag{9}$$

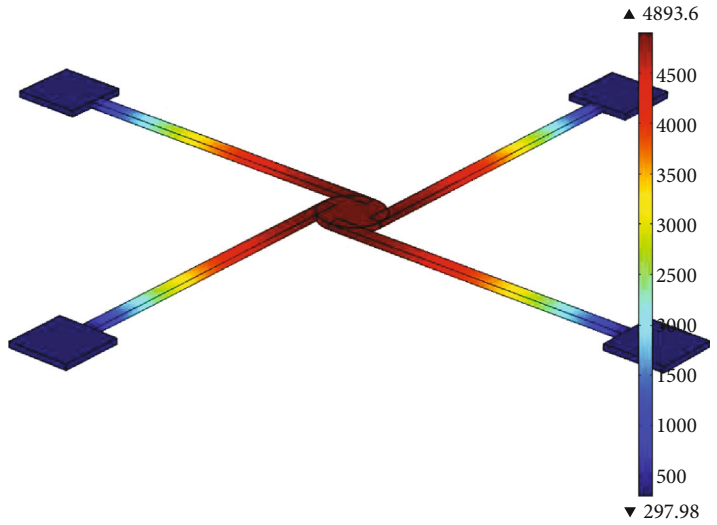

Figure 14: Current density analysis of polysilicon (circular disc 5 μm).

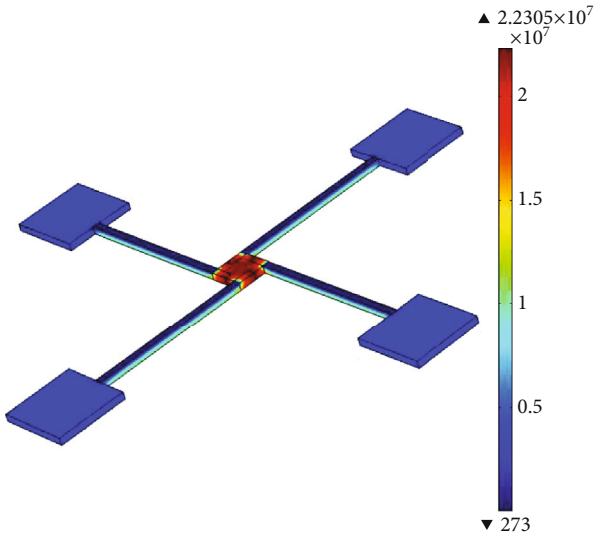

Figure 15: Current density analysis of polysilicon (square arm 10 μm).

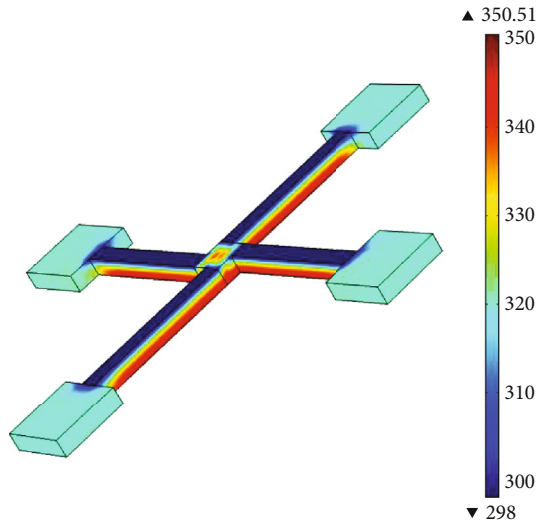

Figure 16: Current density analysis of polysilicon (square arm 25 μm).

where R is the radius of the disc. ΔLh is the total expansion of the free end. δ is the angle of rotation.

Here, taking R as 10 and the angle of rotation as 3.90, then ΔLh = 3900 nm.

4. Results and Discussion

4.1. Stress Analysis. Stress analysis is conducted to find the deformation of microthermal rotary actuator for the given pressure. Normal pressure for the stress analysis is about 7 GPa which is the yield strength of the silicon material and 8.4 GPa for poly silicon.

4.2. Von Mises Stress Analysis. This analysis is used in microthermal rotary actuator. So, when the stress is given, the material starts to yield after the critical value of yield strength which depends on von Mises stress.

4.3. Current Density Analysis. Current density is defined as the amount of charge per unit time that flows through a unit area of a chosen cross-section. Here, expected current density of a MEMS/NEMS thermal rotary actuator should be less than the electric field for fabrication.

4.4. Temperature Analysis. Temperature is a physical property of matter that quantitatively defines hot and cold. It is the indication of thermal energy present in all matter, which is the source of occurrence of heat, which is a flow of energy, when a body is in contact with another one which is cooler. The obtained temperature plot should be less than melting point of the material used there, and the devices is simulated under room temperature 298 K.

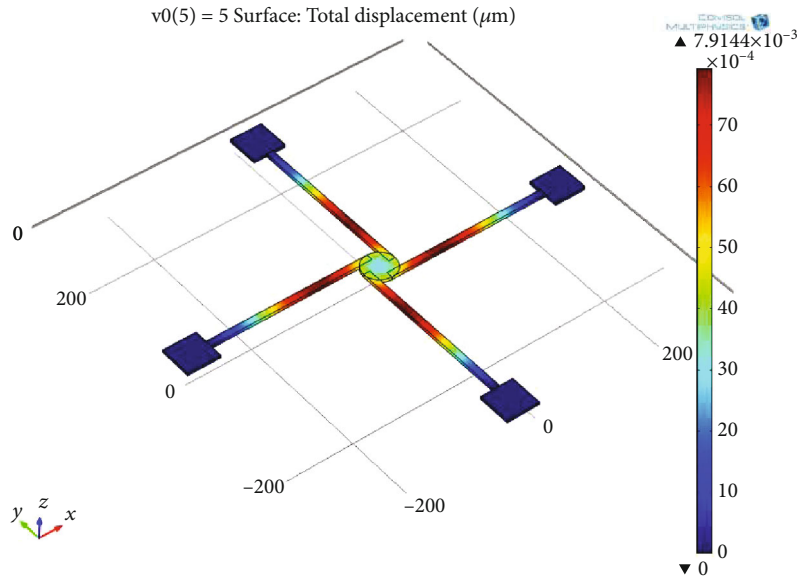

Figure 17: Von Mises stress of silicon (circular disc 5 μm).

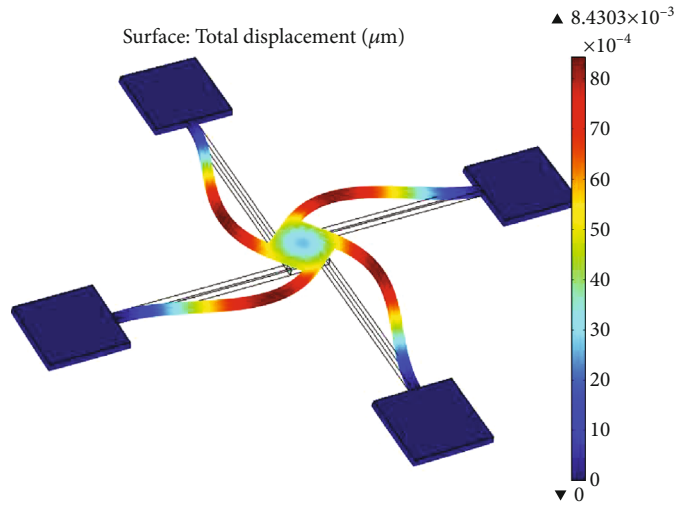

Figure 18: Von Mises stress of silicon (square arm 10 μm).

4.4.1. Temperature Analysis. Figure 5 shows the temperature plot of silicon actuator at room temperature. Here, center arm experiences high heat because the current value is high. Figure 6 shows the temperature of silicon actuator at room temperature.. If the area of the centre arm is increased, temperature is high but less compared to previous square arm of 10 μm. Figure 7 shows the temperature of silicon actuator. The obtained value is 298 K. Polysilicon and silicon are behaving similar in temperature analysis. If the square arm size is 5 μm, temperature developed is so high. Figure 8 shows the temperature of polysilicon actuator. The obtained value varies from 297.98 K to 4893.6 K. As discussed in silicon-based rotary actuator, here, also, if size of arm is increase, then temperature rise is reduced.

Figure 9 shows the temperature of polysilicon actuator. The obtained value varies from 273 K to 2.2305×10^7. Figure 10 shows the temperature of polysilicon actuator. Here, the thickness is increased; hence, heat developed is decreased. The obtained value varies from 298 K to 350.51 K.

4.4.2. Current Density Analysis. Figure 11 shows the current density of silicon actuator. The obtained value is 298. Figure 12 shows the current density of Silicon actuator. The value of bending is 298. Figure 13 shows the current density of silicon actuator. The value of bending varies from 298 to 350.51. Figure 14 shows the current density of poly Si actuator. The value of bending varies from 297.98 to 4893.6. Figure 15 shows the current density of poly silicon actuator.

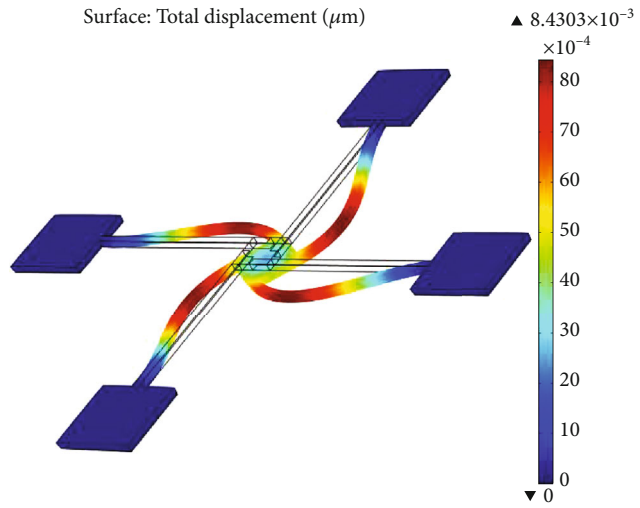

Figure 19: Von Mises stress of silicon (square arm 25 μm).

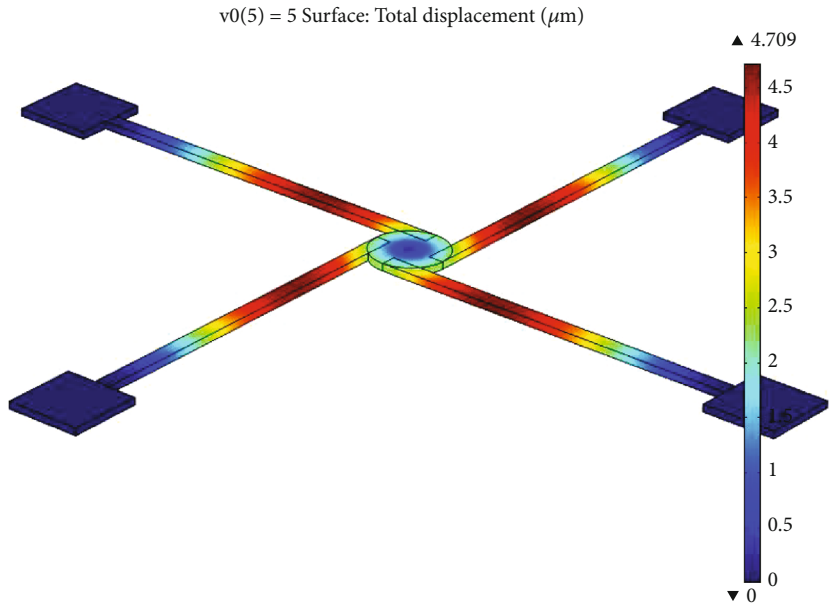

Figure 20: Von Mises stress of polysilicon (circular disc 5 μm).

The value of bending varies from 272 to 2.2307×10^7. Figure 16 shows the current density of poly silicon actuator. The value of bending varies from 272 to 350.

4.4.3. Stress Analysis. Figure 17 shows the von Mises stress of silicon-based actuator. Its range varies from 0 to 7.9144×10^{-9}. Figure 18 shows the von Mises stress of silicon-based actuator. Its range varies from 0 to 8.403×10^{-9}. Figure 19 shows the von Mises stress of silicon-based actuator. Its range varies from 0 to 8.4303×10^{-8}. Figure 20 shows the von Mises stress of polysilicon actuator. The value of bending varies from 0 to 4.709. Figure 21 shows the von Mises stress of silicon-based actuator. Its range varies from 0 to 1.3664×10^4. Figure 22 shows the von Mises stress of silicon-based actuator. Its range varies from 8.0636×10^5 to 4.7792×10^7. Thermal rotary microactuators are a favorable solution to the need for large displacement, low-power MEMS actuators. It is confirmed to be a robust actuation method in surface micromachined devices. Such devices have been used in variety of different applications like

(i) Micromechanical switches

(ii) Micromotors

(iii) Microscale tensile testing

4.4.4. Micro/Nanogear. A micro/NEMS gear is a part of rotating machine which is having cut teeth or, in the case of a cog wheel, it is having inserted teeth (called cogs), which wire with another toothed part which is used to transmit

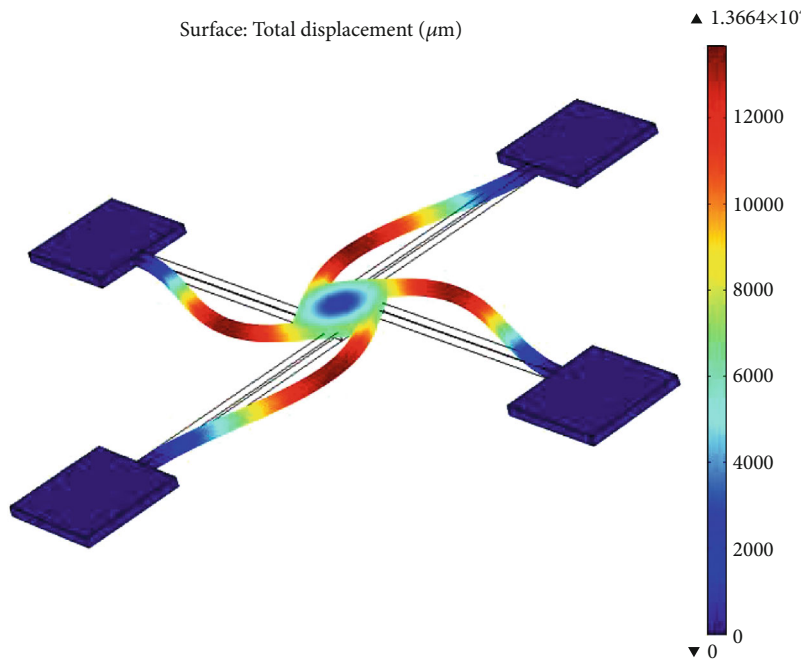

Figure 21: Von Mises stress of polysilicon (square arm 10 μm).

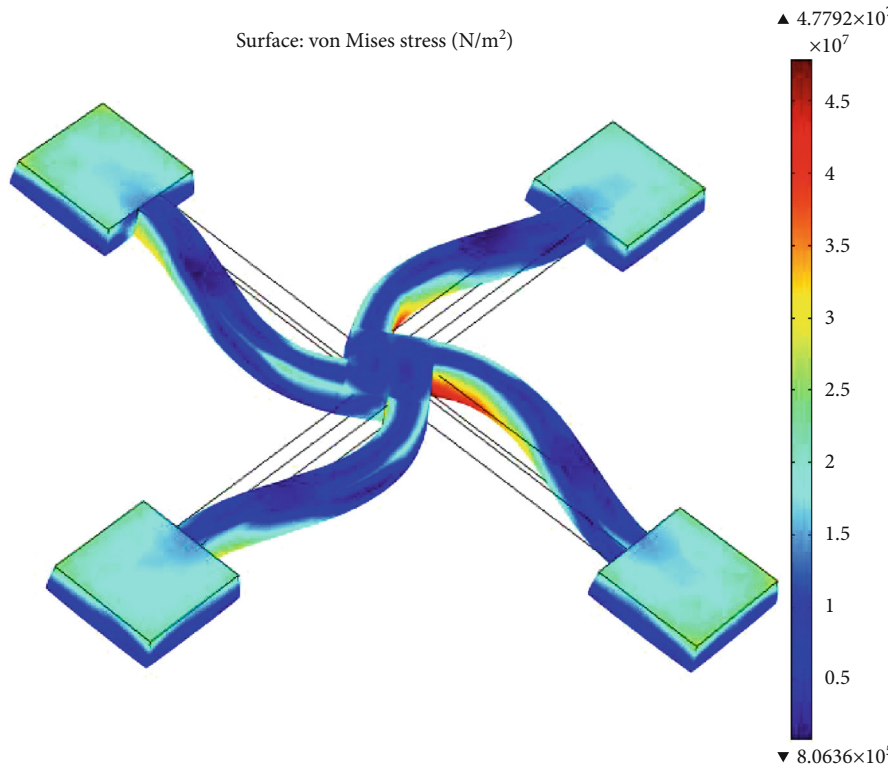

Figure 22: Von Mises stress of polysilicon (square arm 25 μm).

torque. Geared devices can change the speed, torque, and direction of a power source. Gears always used to change torque, through their gear ratio, and they are considered as a simple machine. The teeth on the two interlocked gears have the same shape. Two or more meshing gears, working in a sequence, are called a gear train or a transmission. A gear can mesh with a linear toothed part, called a rack, producing translation instead of rotation.

4.5. Dimension. Microgear design has been done in Figure 23 using the parameters such as inner dimension that is 171 μm and outer dimensions that are 40 μm. The number of teeth is

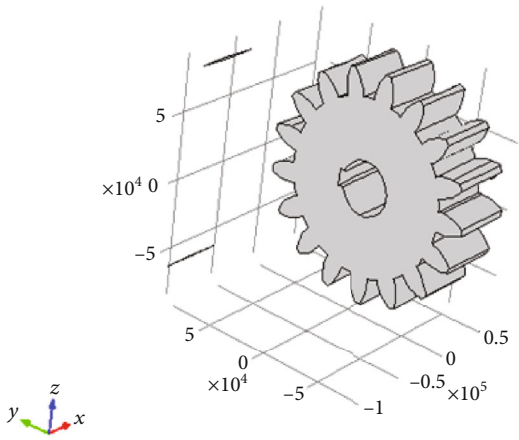

Figure 23: Structure of single microgear.

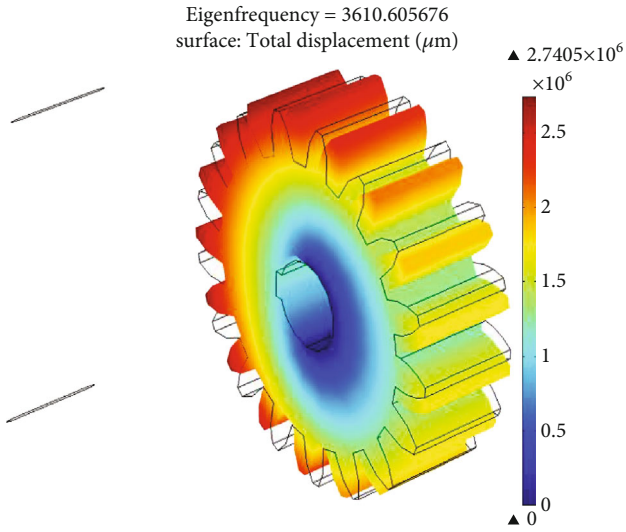

Figure 24: Eigen frequency analysis of micro gear.

17 μm, its width is about 14 μm, and the width is about 50 μm. This design is done by using material called cast iron.

4.6. Eigen Frequency Analysis. When the gear is vibrating at eigen frequency, the gear structure deforms into a corresponding shape which is called eigen mode. An eigen frequency analysis of Figure 24 can only provide the shape of the mode, not the amplitude of the physical vibration. Eigen analysis is done to find the structural behavior of the rotary actuator. If the structure deformation is less, then it is concluded that the designed device will work safely.

5. Conclusion

This work presents the out of plane microthermal rotary actuator with different structures and different dimensions. Stress analysis of microthermal rotary actuator shows its stress bearing capacity for different structures that are different. Current density and temperature analysis show that the safer limit and melting point of the actuator are the same at the every point in the actuator. Also, in microgear eigen frequency analysis is done, it shows that the total displacement of the microgear is same as every point of the design.

Data Availability

The data used to support the findings of this study are included in the article. Should further data or information be required, these are available from the corresponding author upon request.

Conflicts of Interest

The authors declare that there are no conflicts of interest regarding the publication of this paper.

Acknowledgments

The authors appreciate the supports from Bahir Dar Institute of Technology, Bahir Dar University, Ethiopia. The authors thank Saveetha School of Engineering and Vellore Institute of Technology, Chennai, for the technical assistance to support this study.

References

[1] A. Atre and S. Boedo, "Effect of Thermophysical property variations on surface micromachined polysilicon beam flexure actuator," *NSTI-Nanotech*, vol. 2, pp. 263–266, 2004.

[2] A. A. Geisberger, N. Sarkar, M. Ellis, and G. D. Skidmore, "Electrothermal properties and modeling of polysilicon microthermal actuators," *Journal of Microelectromechanical Systems*, vol. 12, no. 4, pp. 513–523, 2003.

[3] S. Heo, G. H. Yoon, and Y. Y. Kim, "The robust design for micro electro-thermal actuators," in *Smart Structures and Materials 2004: Smart Electronics, MEMS, BioMEMS, and Nanotechnology (Vol. 5389, pp. 241-247)*, International Society for Optics and Photonics, 2004.

[4] Q.-A. Huang and N. K. S. Lee, "Analysis and design of polysilicon thermal flexure actuator," *Journal of Micromechanics and Microengineering*, vol. 9, no. 1, pp. 64–70, 1999.

[5] S. Heo and Y. Y. Kim, "Optimal design and fabrication of MEMS rotary thermal actuators," *Journal of Micromechanics and Microengineering*, vol. 17, no. 11, pp. 2241–2247, 2007.

[6] B. Haefner, M. Quiring, J. Gullasch, G. Glaser, T. Dmytruk, and G. Lanza, "Finite element simulation for quality dependent lifetime analysis of micro gears," *Science Direct*, vol. 31, pp. 41–46, 2015.

[7] A. Islam and M. M. Islam, "Stress on spur gear and simulation for micro hybrid systems by Ansys workbench," *Journal of Mechanical and Energy Engineering*, vol. 3, no. 1, pp. 25–30, 2019.

[8] M. A. Arefin, A. Mallik, and M. Asfaquzzaman, "Renewable energy–assisted hybrid three-wheeler: a numerical investigation," *Advances in Mechanical Engineering*, vol. 10, no. 12, Article ID 168781401881437, 2018.

[9] X. Jin, Y. Wang, W. Ju, J. He, and S. Xie, "Investigation into parameter influence of upstream deflector on vertical axis wind turbines output power via three-dimensional CFD simulation," *Renewable Energy*, vol. 115, pp. 41–53, 2018.

[10] A. Arefin and R. Islam, "Investigation of different validation parameters of micro gas turbine for range extender electric

truck," *International Journal of Engineering*, vol. 31, no. 10, pp. 1782–1788, 2018.

[11] S. M. Karbosi, M. Shamshrisar, M. Naraghi, and M. Manoufi, "Optimal design analysis of electrothermally driven microactuators," *Microsystem Technologies*, vol. 16, no. 7, pp. 1065–1071, 2010.

[12] C. Lo, M. Lin, and C. Hwan, "Modeling and analysis of electrothermal microactuators," *Journal of the Chinese Institute of Engineer*, vol. 32, no. 3, pp. 351–360, 2009.

[13] D. Veeman, M. S. Sai, P. Sureshkumar et al., "Additive manufacturing of biopolymers for tissue engineering and regenerative medicine: an overview, potential applications, advancements, and trends," *International Journal of Polymer Science*, vol. 2021, Article ID 4907027, 20 pages, 2021.

[14] R. S. Chiorean, M. C. Dudescu, and M. Pustan, "Analytical and numerical study on the maximum force developed by a V-beam thermal actuator," *Procedia Technology*, vol. 12, pp. 359–363, 2014.

[15] S. Wang, Y. Hao, and S. Liu, "The design and analysis of a MEMS electrothermal actuator," *Journal of Semiconductors*, vol. 36, no. 4, p. 044012, 2015.

[16] A. Potekhina and C. Wang, "Review of Electrothermal Actuators and Applications," *MDPI Actuators*, vol. 8, no. 4, 2019.

[17] Y. Sun, B. D. Leaker, J. E. Lee, R. Nam, and H. E. Naguib, "Shape programming of polymeric based electrothermal actuator (ETA) via artificially induced stress relaxation," *Scientific Reports*, vol. 9, no. 1, article 11445, 2019.

[18] X. Li, Y. Zhao, T. Hu et al., "Design of a large displacement thermal actuator with a cascaded V-beam amplification for MEMS safety-and-arming devices," *Microsystem Technologies*, vol. 21, no. 11, pp. 2367–2374, 2015.

[19] S. Yogeshwaran, L. Natrayan, S. Rajaraman, S. Parthasarathi, and S. Nestro, "Experimental investigation on mechanical properties of epoxy/graphene/fish scale and fermented spinach hybrid bio composite by hand lay-up technique," *Materials Today: Proceedings*, vol. 37, no. 2, pp. 1578–1583, 2021.

[20] S. Kim, W. Kim, and Y. Kim, "Design and performance evaluation of thin-film actuators based on flexible Ni-Co substrates," *Micro and Nano Systems Letters*, vol. 8, no. 1, 2020.

[21] O. Ulkir, "Design and fabrication of an electrothermal MEMS micro-actuator with 3D printing technology," *Materials Research Express*, vol. 7, no. 7, 2020.

[22] H. Steiner, F. Keplinger, J. Schalko, W. Hortschitz, and M. Stifter, "Highly efficient passive thermal micro-actuator," *Journal of Microelectromechanical Systems*, vol. 24, no. 6, pp. 1981–1988, 2015.

[23] N. T. Duzng, "Modeling and simulation of V-shaped thermal actuator," *American Journal of Engineering Research*, vol. 7, no. 4, pp. 222–227, 2018.

[24] M. Li, Z. Zhou, L. Yi, X. Wang, and S. Adnan, "Design of a test structure based on chevron-shaped thermal actuator for in-situ measurement of the fracture strength of MEMS thin films," *Nanotechnology and Precision Engineering*, vol. 2, no. 4, pp. 163–168, 2019.

[25] R. Suryanarayanan, V. G. Sridhar, L. Natrayan et al., "Improvement on mechanical properties of submerged friction stir joining of dissimilar tailor welded aluminum blanks," *Advances in Materials Science and Engineering*, vol. 2021, Article ID 3355692, 6 pages, 2021.

[26] Y. J. Gong, F. Zhao, H. Y. Xiang, and L. Zhang, "Thermal analysis and simulation of MEMS thermal actuator for food industry," *Advanced Materials Research*, vol. 179-180, pp. 392–397, 2011.

[27] B. López-Walle, M. Gauthier, and N. Chaillet, "Dynamic modelling for thermal micro-actuators using thermal networks," *International Journal of Thermal Sciences*, vol. 49, no. 11, pp. 2108–2116, 2010.

[28] D. H. Kim, K. S. Oh, and S. Park, "Design and analysis of a twisting-type thermal actuator for micromirrors," *Journal of Mechanical Science and Technology*, vol. 23, no. 6, pp. 1536–1543, 2009.